Structure-Based Design of Potent Inhibitors of Scytalone Dehydratase: Displacement of a Water Molecule from the Active Site‡

James M. Chen,*,§,|| Simon L. Xu,§ Zdzislaw Wawrzak,⊥ Gregory S. Basarab,§ and Douglas B. Jordan*,§

E. I. DuPont de Nemours Agricultural Products, Stine-Haskell Research Center, P.O Box 30, Newark, Delaware 19714, and E. I. DuPont de Nemours Central Research and Development, Experimental Station, Wilmington, Delaware 19880-0228

Received August 3, 1998; Revised Manuscript Received October 21, 1998

ABSTRACT: Scytalone dehydratase (SD) is a molecular target of inhibitor design efforts aimed at protecting rice plants from the fungal disease caused by *Magnaporthe grisea*. As determined from X-ray diffraction data of an SD−inhibitor complex [Lundqvist et al. (1994) *Structure (London) 2*, 937−944], there is an extended hydrogen-bonding network between protein side chains, the inhibitor, and two bound water molecules. From models of SD complexed to quinazoline and benztriazine inhibitors, a new class of potent SD inhibitors involving the displacement of an active-site water molecule were designed. We were able to increase inhibitory potency by synthesizing compounds with a nitrile functionality displayed into the space occupied by one of the crystallographic water molecules. Sixteen inhibitors are compared. The net conversion of potent quinazoline and benztriazine inhibitors to cyanoquinolines and cyanocinnolines increased binding potency 2−20-fold. Replacement of the nitrile with a hydrogen atom lowered binding affinity 100−30 000-fold. X-ray crystallographic data at 1.65 Å resolution on a SD−inhibitor complex confirmed that the nitrile functionality displaced the water molecule as intended and that a favorable orientation was created with tyrosines 30 and 50 which had been part of the hydrogen-bonding network with the water molecule. Additional data on inhibitors presented herein reveals the importance of two hydrogen-bonding networks toward inhibitory potency: one between Asn131 and an appropriately positioned inhibitor heteroatom and one between a bound water molecule and a second inhibitor heteroatom.

The use of X-ray crystallography of protein complexes has gained widespread acceptance for the design and optimizations of ligands of importance for pharmaceutical and agrochemical utilities (*1*, *2*). Marked advancements in molecular biology, X-ray crystallographic equipment, and computer technology has led to an exponential growth in the number of protein and other biomacromolecular structures being solved. The models derived from the crystallography experiments allow the medicinal chemist to design molecules from the consideration of the interactions within the enzyme-binding pocket. We now report insights from the structure of scytalone dehydratase (SD, EC 4.2.1.94)[1] for improving binding potency of a new class of inhibitors. SD catalyzes two steps (*3*) in the melanin biosynthetic pathway of the plant pathogen *Magnaporthe grisea* (Figure 1), the causative agent of blast disease in rice crops. This pathway begins with the oligomerization of acetate to a pentaketide and cyclization to tetrahydroxynaphthalene. A series of reductions and dehydrations (the latter catalyzed by SD) converts tetrahydroxynaphthalene to dihydroxynaphthalene which is the ultimate precursor to fungal melanin. In *M. grisea*, fungal melanin is absolutely required for infection of its host rice leaves (*4*, *5*), and therefore, the biosynthetic pathway enzymes are attractive targets for fungicide design. Furthermore, since the biosynthetic pathway does not exist in mammalian or plant systems, the potential for off-target toxicity with chemistry that would block fungal melanin production is lowered.

The X-ray crystal structure of SD from *M. grisea* in complex with salicylamide inhibitor **1a** (*6*) became the starting point for our inhibitor design strategy. Inhibitor **1a** exhibits an extensive hydrogen-bonding network with the protein and two bound water molecules (see Figure 2A) in addition to many hydrophobic interactions with protein side chains (not shown). The hydrogen-bonding network as diagrammed in Figure 2A corresponds to one we believe best accounts for the binding potency of the inhibitor. However, the hydrogen bonds between the active site residues, the water molecules, and the inhibitor should be considered to have dynamic character. One of the crystallographic water molecules is positioned within the binding pocket to form hydrogen bonds with the salicylamide carbonyl oxygen atom and with the phenolic hydroxyls of tyrosines 30 and 50. This water molecule has been postulated to serve as a general acid in conjunction with the two tyrosine residues to induce enolization of substrate scytalone (*6*, *7*).

‡ Atomic coordinates for the SD-inhibitor complex described herein have been deposited in the Brookhaven Protein Data Bank (accession code 3STD).

* To whom correspondence should be addressed. E-mail: doug.b.jordan@usa.dupont.com and WAPR12.JM@war.wyeth.com.

§ E. I. DuPont de Nemours Agricultural Products.

|| Present address: Wyeth-Ayerst Research, Computational Chemistry, Building 222, 401 Middletown Road, Pearl River, NY 10965.

⊥ E. I. DuPont de Nemours Central Research and Development.

[1] Abbreviations: SD, scytalone dehydratase; Tris, tris(hydroxymethyl)aminomethane; DDBO, 2,3-dihydro-2,5-dihydro-4H-benzopyran-4-one; DMSO, dimethyl sulfoxide; PEG, poly(ethylene glycol); 1STD, the PDB accession code for the original X-ray structure of SD complexed with inhibitor **1a**.

10.1021/bi981848r CCC: $15.00
Published on Web 12/03/1998

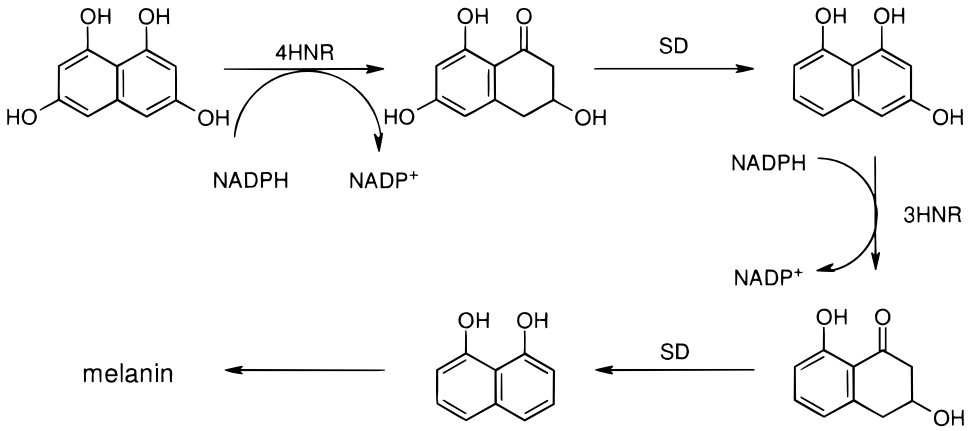

FIGURE 1: The fungal melanin biosynthetic pathway. 4HNR = tetrahydroxynaphthalene reductase; SD = scytalone dehydratase; 3HNR = trihydroxynaphthalene reductase.

The second water molecule, which forms hydrogen bonds with the NH of the inhibitor and the ϵ-nitrogen atoms of histidines 85 and 110, has been implicated as the water of dehydration in the SD catalytic cycle (*6*). We have reason to believe that if we replaced the salicylamide portion of **1a** with a nearly isosteric quinazoline heterocycle, the hydrogen-bonding network involving the two water molecules would be maintained. The ability of the quinazoline heterocycle to mimic the ring resulting from the intramolecular hydrogen bond of salicylamides such as **1a** in the context of inhibiting SD catalytic activity has been published (*8*). It was anticipated that the 1-position nitrogen atom of the quinazoline ring would occupy the position of the hydroxyl of **1a** to receive a hydrogen bond from the side chain of Asn131. Upon completion of the work outlined in this paper, the X-ray crystal structure of SD bound with a quinazoline inhibitor was solved at high resolution (Z. Wawrzak, T. Sandolova, J. Steffens, G. Basarab, T. Lundqvist, Y. Lindqvist, and D. Jordan, unpublished results) and, as predicted, the two inhibitor-associated water molecules are maintained as is the hydrogen bond from inhibitor to Asn131. Importantly, an appropriate bulky hydrophobic substituent is needed on the amino group to occupy a cavity lined with a number of hydrophobic amino acid side chains in order to achieve potent inhibition. We reasoned that fused heterocycles could serve as suitable scaffolds for introduction of functionalities that might displace one of the crystallographic active-site water molecules.

The benefits in binding efficacy that might be gained by displacement of such a water molecule are well recognized in the literature (*9*−*15*). First, there is a gain in entropy by freeing the water molecule from a constrained environment to bulk solvent. Second, there is the potential to build a binding interaction directly with the protein residues that coordinated the water molecule. This second point is important as the steric and electronic environment for binding the water molecule must offer an enthalpic contribution to the overall free energy of the system that is greater than the entropic penalty due to constraining the water molecule. Otherwise, the water molecule would not be so constrained. If inhibitor analogues are designed to displace a bound water molecule, the loss of enthalpic stabilization due to the water molecule should be regained, in part, with an enthalpic contribution from the designed inhibitor.

The evolution of our design of SD inhibitors can be exemplified by the sequence shown in Figure 3. The quinazoline and benztriazine rings of **2** and **5**, respectively, serve as isosters for the salicylamide **1**. Figure 2, panels B and C, diagrams the orientations of the quinazoline and benztriazine inhibitors relative to the key binding pocket residues as modeled. The two water molecules associated with the salicylamide inhibitors were retained within these SD−inhibitor models. Replacing the quinazoline and benztriazine 3-position nitrogens with a carbon atom allows for a substituent X to occupy the position of the water molecule situated between Tyr30 and Tyr50. The region of the binding pocket around this water molecule is rather small, and large R substituents are not expected to be tolerated. Allowing R to be CN is appealing since it is relatively small and the triple bond π-electrons could accept an albeit weak hydrogen bond from the tyrosine hydroxyls (*16*). The 1-position nitrogen of the quinoline and benztriazine rings are oriented to receive a hydrogen bond from Asn131 and the nitrile takes the place of the water molecule associated with Tyr30 and Tyr50. We synthesized a series of amino quinolines and amino cinnolines with a CN substituent at the 3-position for evaluation as SD inhibitors to determine whether we could indeed displace an associated water molecule while gaining inhibitor potency. For comparison, we also synthesized the parent quinolines **3** and cinnolines **6** (X = H, Figure 3). Finally, we synthesized phthalazines **8** (Scheme 1) to quantify the importance of maintaining a hydrogen bond accepting heteroatom adjacent to the Asn131 side-chain amide.

MATERIALS AND METHODS

Materials. Homogeneous wild-type scytalone dehydratase was purified as described (*17*). Construction and purification of N-truncated scytalone dehydratase will be described elsewhere. DDBO was synthesized as described (*18*). All other materials were from Aldrich Chemical (Milwaukee, WI), Sigma Chemical (St. Louis, MO), Hampton (Laguna Hills, CA), Fluka (Buchs, Switzerland), ICN Biomedicals, Inc. (Costa Mesa, CA), or Lancaster Synthesis Inc. (Windham, NH).

*Computer Models of SD Complexed to **2a** and to **5a**.* Molecular modeling was carried out using the Sybyl molecular modeling package from Tripos, Inc. (St. Louis, MO) on a Silicon Graphics Inc. Indigo. The 3D structure of the

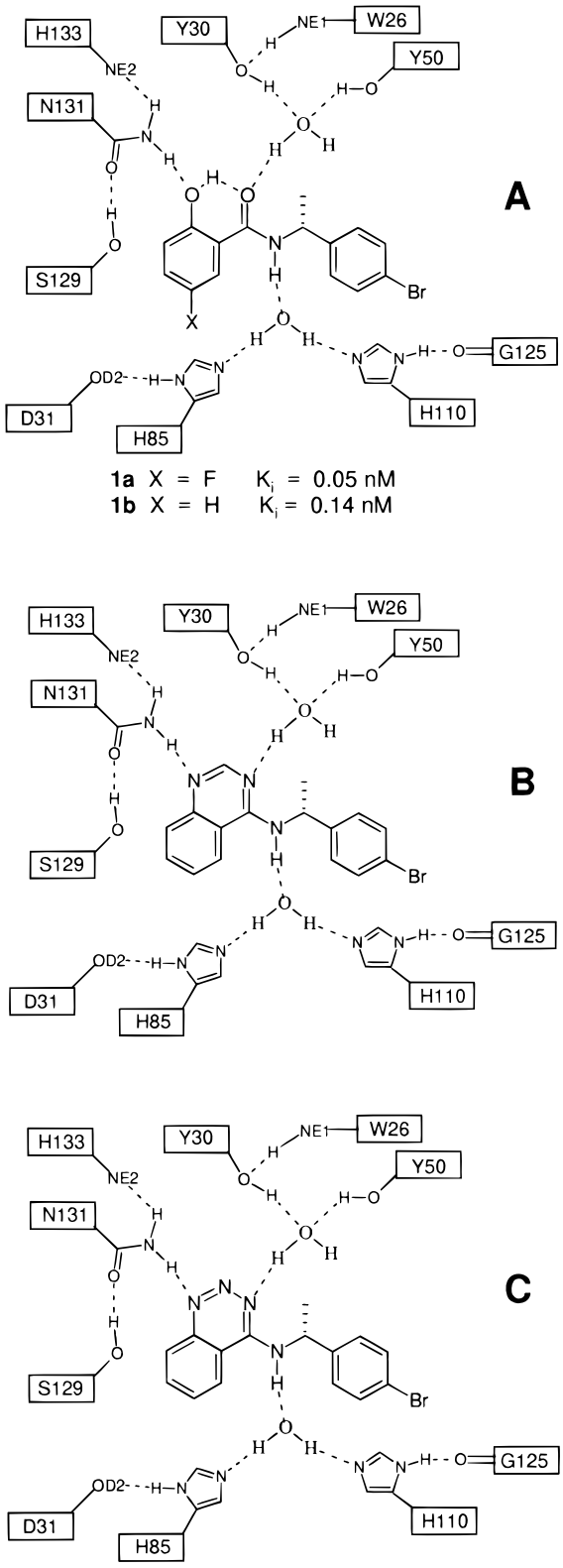

FIGURE 2: (A) Interactions of salicylamide inhibitors with key residues in the scytalone dehydratase binding pocket as given by crystallographic data for **1a**. (B) Interactions of quinazoline **2e** with key residues in the scytalone dehydratase binding pocket as modeled. (C) Interactions of benztriazine **5a** with key residues in the scytalone dehydratase binding pocket as modeled.

salicylamide inhibitor **1a** complexed to SD (1STD) (*6*) was removed from the protein and modified graphically to **2a** and **5a**. Each inhibitor was then merged back into the active-site of SD, forming two new complexes. To relax the strain energies produced by the modified inhibitors, each SD−inhibitor model was optimized utilizing a set of nested refinement procedures involving energy minimization (*19*). A Connolly solvent-accessible surface was generated with the MOLCAD algorithm from Tripos, Inc. using a 1.3 Å probe while selecting 29 residues that line the binding pocket and removing the inhibitor and the two associated water molecules.

Synthesis of (R)-N-[1-(4-Bromophenyl)ethyl]-4-quinazolinamine **2a**. A solution of 0.5 g (3.1 mmol) of 4-chloroquinazoline (*20*), 0.67 g (3.3 mmol) of (*R*)-1-(4-bromophenyl)-ethylamine (Lancaster), and 0.73 mL (6.7 mmol) of triethylamine in 30 mL of glyme was heated at reflux overnight. Solvent was removed and the residue was dissolved in ethyl acetate, washed with water and brine, and dried ($MgSO_4$). Removal of solvent was followed by chromatography on silica gel (4:1 hexanes−ethyl acetate) affording 560 mg of **2a** as a white solid, mp 144−145 °C. ^{1}H NMR (300 MHz, $CDCl_3$): δ 1.7 (d, J = 7 Hz, 3H), 5.6 (m, 1H), 5.8 (d, J = 5 Hz, 1H), 7.3 (d, J = 6 Hz, 2H), 7.5 (m, 3H), 7.75 (m, 2H), 8.85 (d, J = 6 Hz, 1H), 8.6 (s, 1H).

Synthesis of N-(3,3-Diphenypropyl)-4-quinazolinamine **2d**. Following the procedure for the preparation of compound **2a**, 1.0 g (6.1 mmol) of 4-chloroquinazoline, 1.4 g (6.7 mmol) of 3,3-diphenylpropylamine (Aldrich), and 1.35 g (13.4 mmol) of triethylamine reacted to afford 1.2 g of compound **2d** as a white solid, mp 149−152 °C. ^{1}H NMR (300 MHz, $CDCl_3$): δ 2.55 (q, J = 7 Hz, 2H), 3.75 (q, J = 7 Hz, 2H), 4.1 (t, J = 7 Hz, 1H), 5.5 (s, 1H), 7.2−7.35 (m, 11H), 7.4 (t, J = 6 Hz, 1H), 7.7 (t, J = 6 Hz, 1H), 7.8 (d, J = 6 Hz, 1H), 8.1 (s, 1H).

Synthesis of N-(3,3-Diphenypropyl)-4-quinolinamine **3d**. A solution of 1.0 g (6.4 mmol) of 4-chloroquinoline (Aldrich) and 1.3 g (6.4 mmol) of 3,3-diphenylpropylamine in 30 mL of *n*-pentanol was heated at reflux overnight. Solvent was removed, and the residue was partitioned between ethyl acetate and water. The ethyl acetate was separated, washed with brine, and dried ($MgSO_4$). Removal of solvent and chromatography on silica gel (4:1 hexanes−ethyl acetate) gave 1.23 g of a white solid, mp 142−144 °C. ^{1}H NMR (300 MHz, $CDCl_3$): δ 2.55 (q, J = 7 Hz, 2H), 3.4 (q, J = 7 Hz, 2H), 4.1 (t, J = 7 Hz, 1H), 4.9 (m, 1H), 6.3 (d, J = 5 Hz, 1H), 7.2−7.5 (m, 12H), 7.6 (t, J = 6 Hz, 1H), 7.95 (d, J = 6 Hz, 1H), 8.5 (d, J = 5 Hz, 1H).

Synthesis of (R)-N-[1-(4-Bromophenyl)ethyl]-2-cyano-4-quinolinamine ***4a***. A solution of 0.20 g (1.06 mmol) of 4-chloro-3-cyanoquinoline (*21*), 0.43 g (2.12 mmol) of (*R*)-1-(4-bromophenyl)ethylamine, 0.44 g (3.18 mmol) of K_2CO_3, and 20 mg of KI in 5 mL of DMF was heated at reflux for 4 h. The reaction was worked up by quenching with water and extracting with ethyl acetate. Removal of solvent gave a brown oil which was purified by chromatography using 4:1 hexanes−ethyl acetate to give 0.36 g of product as an off-white solid, mp 130−132 °C. ^{1}H NMR (300 MHz, $CDCl_3$): δ 1.7−1.75 (m, 3H), 5.9 (m, 1H), 7.25−7.3 (m, 1H), 7.45−7.50 (m, 4H), 7.8 (m, 2H), 8.0 (m, 2H), 8.5 (m, 1H).

Synthesis of N-(3,3-Diphenypropyl)-2-cyano-4-quinolinamine ***4d***. Following the procedure for the preparation of compound **4a**, 0.17 g (0.9 mmol) of 4-chloro-3-cyanoquinoline and 0.38 g (1.8 mmol) of 3,3-diphenylpropylamine reacted to give 270 mg of product as a waxy solid, mp 125−

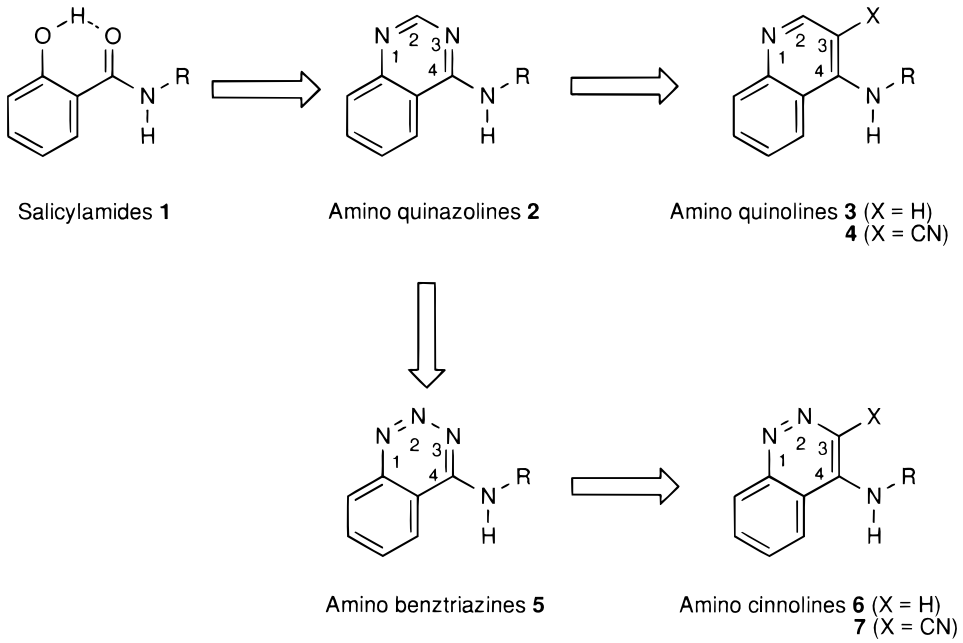

FIGURE 3: Design sequence for inhibitors of scytalone dehydratase.

Scheme 1: Synthesis of Inhibitors

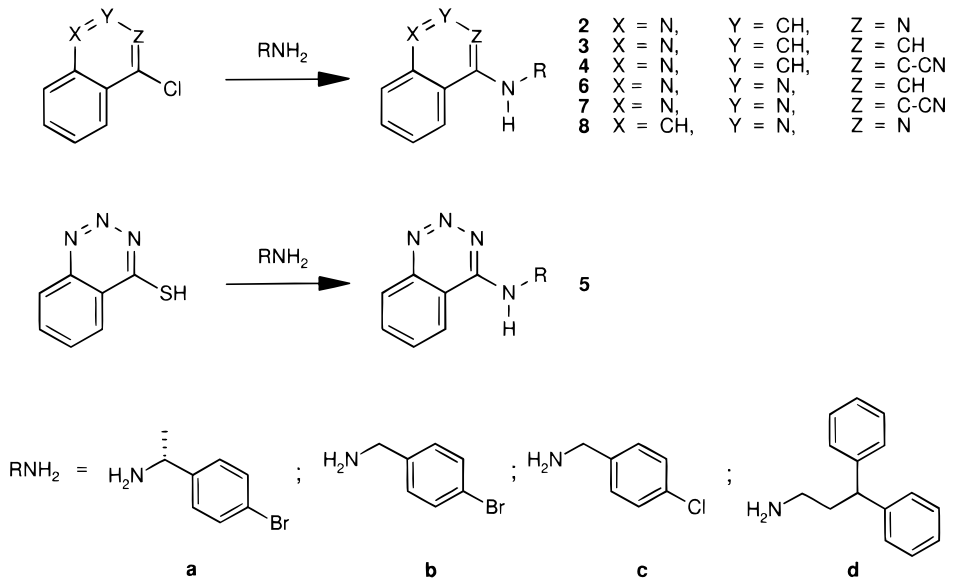

127 °C. ^{1}H NMR (300 MHz, $CDCl_3$): δ 2.6−2.65 (m, 2H), 3.95−4.05 (m, 2H), 4.1−4.2 (m, 1H), 5.2 (m, 1H), 7.1−7.15 (m, 1H), 7.15−7.30 (m, 10H), 7.3−7.40 (m, 1H), 7.6−7.7 (m, 1H), 7.9−7.95 (m, 1H), 8.55 (s, 1H).

Synthesis of N-[1-(4-Bromophenyl)ethyl]-benz-1,2,3-triazin-4-amine ***5a***. A solution of 0.5 g (3.4 mmol) of 1,2,3-benzotriazine-4(1H)-thione (*22*) and 0.82 g (4.1 mmol) of (*R*)-1-(4-bromophenyl)ethylamine in 15 mL of *n*-butanol was heated at reflux overnight. Solvent was removed, and the residue was chromatographed on silica gel (4:1 hexanes−ethyl acetate) giving a white solid, mp 174−176 °C. ^{1}H NMR (300 MHz, $CDCl_3$): δ 1.7 (d, J = 7 Hz, 3H), 5.8 (m, 1H), 6.0 (d, J = 5 Hz, 1H), 7.3 (d, 2H), 7.45 (t, 1H), 7.75 (t, J = 6 Hz, 1H), 7.8−8.0 (m, 2H), 8.2 (d, J = 6 Hz, 1H).

Synthesis of N-(3,3-Diphenypropyl)-4-benz-1,2,3-triazinamine ***5d***. Following the procedure for the preparation of compound **5a**, 0.5 g (3.4 mmol) of 2,3-benzotriazine-4(1H)-thione and 0.86 g (4.1 mmol) of 3,3-diphenylpropylamine reacted to afford 630 mg of compound **5d** as a white solid, mp 198−199 °C. ^{1}H NMR (300 MHz, $CDCl_3$): δ 2.6 (q, J = 7 Hz, 2H), 3.9 (q, J = 7 Hz, 2H), 4.1 (t, J = 7 Hz, 1H), 5.35 (m, 1H), 7.2 (m, 2H), 7.25−7.35 (m, 9H), 7.7 (t, J = 6 Hz, 1H), 7.9 (t, J = 6 Hz, 1H), 8.2 (d, J = 5 Hz, 1H).

Synthesis of N-[(4-Bromophenyl)methyl]-4-cinnolinamine ***6b***. To a flask charged with 0.20 g (1.2 mmol) of 4-chlorocinnoline (*23*) in 6 mL of DMF was added 0.81 g (3.6 mmol) of 4-bromobenzylamine hydrochloride, 1.0 g (7.2 mmol) of K_2CO_3, and 20 mg of KI. The resulting mixture was heated at reflux for 4 h. The reaction was worked up by adding 10 mL of water and extracted with ether. The organic layers were dried ($MgSO_4$) and concentrated to give an orange oil which was purified by silica gel chromatography using 20:1 hexanes−ethyl acetate as the eluant to give a solid which was further triturated with ether to give 240 mg of product as a white solid, mp 212−215 °C. ^{1}H NMR (300 MHz, $CDCl_3$): δ 4.6 (d, J = 5.4 Hz, 2H), 5.1 (s, 1H),

7.3 (d, $J = 8.4$ Hz, 2H), 7.5 (d, $J = 8.4$ Hz, 2H), 7.6−7.65 (m, 1H), 7.75−7.80 (m, 2H), 8.4 (d, $J = 8$ Hz, 1H), 8.7 (s, 1H).

*Synthesis of N-[(4-Chlorophenyl)methyl]-4-cinnolinamine **6c***. Following the procedure for the preparation of compound **6b**, 0.30 g (1.8 mmol) of 4-chlorocinnoline and 0.77 g (5.4 mmol) of 4-chlorobenzylamine (Aldrich) reacted to form 280 mg of compound **6c** as a white solid, mp 155−159 °C. ^{1}H NMR (300 MHz, $CDCl_3$): 4.6 (d, $J = 5$ Hz, 2H), 5.35 (s, 1H), 7.25−7.4 (m, 4H), 7.60−7.65 (m, 1H), 7.75−7.8 (m, 2H), 8.35−8.4 (m, 1H), 8.7 (s, 1H).

*Synthesis of N-(3,3-Diphenylpropyl)-4-cinnolinamine **6d***. Following the procedure for the preparation of compound **6b**, 0.20 g (1.2 mmol) of 4-chlorocinnoline and 0.77 g (3.6 mmol) of 3,3-diphenylpropylamine reacted to form 320 mg of compound **6d** as a white solid, mp 183−187 °C. ^{1}H NMR (300 MHz, $CDCl_3$): 2.5−2.6 (m, 2H), 3.4−3.45 (m, 2H), 4.0−4.1 (m, 1H), 5.3 (s, 1H), 7.2−7.3 (m, 10H), 7.5−7.55 (m, 2H), 7.7−7.75 (m, 1H), 8.25−8.3 (m, 1H), 8.53 (s, 1H).

*Synthesis of 3-Cyano-N-(3,3-diphenylpropyl)-4-cinnolinamine **7d***. A solution of 0.25 g (1.32 mmol) of 4-chloro-3-cyanocinnoline (*24*), 0.56 g (2.64 mmol) of 3,3-diphenylpropylamine, 0.36 g (2.64 mmol) of K_2CO_3, and 10 mg of KI in 5 mL of DMF was heated at 100 °C for 6 h. It was cooled to room temperature and diluted with water. A tan solid formed which was collected and purified by silica gel column chromatography using 3:1 hexanes−ethyl acetate as the solvent to give product as a pale yellow solid (0.30 g, 63%), mp 215−220 °C. ^{1}H NMR (300 MHz, $CDCl_3$): 2.6 (q, $J = 7.3$ Hz, 2H), 4.05 (q, $J = 7.3$ Hz, 2H), 4.15 (t, $J = 7.0$ Hz, 1H), 5.2 (s, 1H), 7.15 (d, $J = 6.8$ Hz, 1H), 7.25−7.3 (m, 10H), 7.6 (t, $J = 7.0$ Hz, 1H), 7.85 (t, $J = 7.0$ Hz, 1H), 8.39 (d, $J = 6.8$ Hz, 1H).

*Synthesis of (R)-3-Cyano-N-[1-(4-bromophenyl)ethyl]4-cinnolinamine **7a***. Following the procedure for the preparation of compound **7d**, 0.25 g (1.32 mmol) of 4-chloro-3-cyanocinnoline and 0.31 g (1.6 mmol) of (*R*)-1-(4-bromophenyl)ethylamine reacted to give 250 mg of compound **7a** as an off-white solid, mp 205−206 °C, ^{1}H NMR (300 MHz, acetone-d_6): 1.8 (d, $J = 6.0$ Hz, 3H), 5.95 (q, $J = 6.0$ Hz, 1H), 7.5−7.6 (m, 4H), 7.85−7.9 (m, 1H), 8.0−8.05 (m, 1H), 8.35 (d, $J = 6.7$ Hz, 1H), 8.6 (d, $J = 6.7$ Hz, 1H).

*Synthesis of 3-Cyano-N-[(4-bromophenyl)methyl]-4-cinnolinamine **7b***. Following the procedure for the preparation of compound **7d**, 0.23 g (1.2 mmol) of 4-chloro-3-cyanocinnoline and 0.45 g (2.4 mmol) of 4-bromobenzylamine reacted to give 230 mg of compound **7b** as a pale yellow solid, mp 235−240 °C. ^{1}H NMR (300 MHz, $CDCl_3$): 5.1 (d, $J = 5.0$ Hz, 2H), 5.5 (s, 1H), 7.3 (d, $J = 7.0$ Hz, 2H), 7.6 (d, $J = 7.0$ Hz, 2H), 7.7−7.9 (m, 3H), 8.45−8.5 (m, 1H).

*Synthesis of 3-Cyano-N-[(4-chlorophenyl)methyl]-4-cinnolinamine **7c***. Following the procedure for the preparation of compound **7d**, 0.30 g (1.6 mmol) of 4-chloro-3-cyanocinnoline and 0.77 g (3.6 mmol) of 4-chlorobenzylamine reacted to give 240 mg of compound **7c** as a pale yellow solid, mp 229−231 °C. ^{1}H NMR (300 MHz, $CDCl_3$): 5.1 (d, $J = 5.0$ Hz, 2H), 5.6 (s, 1H), 7.3−7.4 (m, 4H), 7.7−7.8 (m, 1H), 7.8 (d, $J = 7.5$ Hz, 1H), 7.90−7.95 (m, 1H), 8.5 (d, $J = 7.5$ Hz, 1H).

*Synthesis of N-[(4-Bromophenyl)methyl]-1-phthalazinamine **8b***. A small quantity of **8b** was prepared by heating a mixture of 2-chlorophthalazine (ICN), 1.2 equiv of 4-bromobenzylamine hydrochloride (Aldrich), 3.0 equiv of K_2CO_3, and a catalytic amount of KI. The mixture was cooled to room temperature and quenched with water and extracted with ether. The organic phase was dried ($MgSO_4$) and concentrated to give an oil. The oil was purified by silica gel column chromatography using 15:1 hexanes−ethyl acetate. ^{1}H NMR (400 MHz, $CDCl_3$): 4.75 (s, 2H), 7.2 (d, $J = 8.0$ Hz, 2H), 7.5 (d, $J = 8.0$ Hz, 2H), 7.6 (d, $J = 8.5$ Hz, 2H), 7.6 (d, $J = 8.5$ Hz, 2H), 8.3 (s, 1H).

*Synthesis of N-(3,3-dipheylpropyl)-1-phthalazinamine **8d***. A mixture of 1.0 g (6.1 mmol) of 2-chlorophthalazine, 3.8 g (18.2 mmol) of 3,3-diphenylpropylamine, 1.7 g (12.2 mmol) of K_2CO_3, and 20 mg of KI was heated at reflux for 16 h. The mixture was cooled to room temperature and quenched with water and extracted with ether. The organic phase was dried ($MgSO_4$) and concentrated to give an orange oil which was purified by silica gel column chromatography (5:1 hexanes−ethyl acetate) to give **8d** as a white solid, mp 134−136 °C. ^{1}H NMR (400 MHz, $CDCl_3$): δ 2.55−2.62 (m, 2H), 3.8−3.85 (m, 2H), 4.1 (t, $J = 7.0$ Hz, 1H), 4.9 (s, 1H), 7.15−7.2 (m, 2H), 7.25−7.3 (m, 9H), 7.7−7.80 (m, 3H), 8.9 (s, 1H).

Determination of Inhibition Constants. Method A. Assay mixtures (1 mL) included 100 mM sodium phosphate, 0.2−1.0 mM DBBO (the latter concentration, approximately 67-fold larger than the K_m for the substrate), 0.5% DMSO, and 0.6 nM SD at pH 7.0 and 25 °C. Reactions (30 s) were initiated with SD and monitored continuously at 320 nM by using an HP 8542A spectrophotometer (Hewlett-Packard). Initial rates were determined from the instrument's software fittings to a line which is valid since the traces were linear and since the results indicated that even the tightest-binding inhibitors had no apparent time dependencies in these assays or ones which had longer time courses. K_i values were determined by fitting the data to eq 1 describing competitive inhibition (*25*). V is the velocity of reactions in the absence of inhibitor, A is the substrate concentration, K is the Michaelis constant for substrate DDBO ($K = 15$ μM from numerous determinations), I is the inhibitor concentration, and K_i is the dissociation constant for the inhibitor from binary SD−inhibitor complex. Inhibitor concentrations in the assays were at least 5-fold in excess of the enzyme concentration in all cases so the enzyme concentration term was omitted from consideration. Nonlinear least-squares fits to eq 1 were through the computer program RS1 (BBN Research Systems; Cambridge, MA).

$$v = \frac{VA}{A + K(I/K_i)} \tag{1}$$

Method B. Determinations of K_is were identical as in method A with the following exceptions: enzyme concentration was increased to 3.0 nM and initial rates were determined over a 10 s time course. Method B was employed for the inhibitors having weaker binding constants.

*Crystallization, Data Collection, and Refinement on SD−**7d***. X-ray crystal studies of SD−inhibitor complexes were determined by using a N-truncated form of the enzyme (lacking residues 3−9) and modified crystallization protocols. Crystallization conditions for enzyme in complex with **7d** were 0.1 M Tris-HCl, pH 7.5, 200−250 mM $CaCl_2$, and 32−

34% PEG 400 in sitting or hanging drops. X-ray data was collected at 100 K on a RAXIS-IV imaging plate system with CuKα X-rays from a Rigaku rotating anode generator. Prior to data collection, crystals were mounted on nylon loops with a diameter of 0.3−0.5 mm, washed briefly in well solution, and directly frozen in the 100 K cold stream generated by an Xstream cryosystem (Molecular Structure Corp., The Woodlands, TX).

The program AMoRe (*26*) was employed to calculate the orientation and position of the SD trimer within the unit cell by using the model of 1STD (*6*) as the search model. The structures were refined with the program X-PLOR (*27, 28*) beginning with the simulated annealing protocol between 3000 and 300 K followed by several positional and *B*-factor refinement cycles. A portion (7.5%) of the data was omitted from the refinement cycles for calculations of R-free values (*29*). Water molecules were added to well-defined peaks (2.0σ and greater in $F_o - F_c$ maps) found between 2 and 4 Å from O or N atoms in the protein. Within the set of water molecules, those having very low *B*-factors and residual density were examined as possible calcium ions, and if there were appropriate interactions with amino acid residues, they were refined as calcium ions.

RESULTS AND DISCUSSION

Synthesis. The amino heterocyclic compounds **2**, **3**, **4**, **6**, **7**, and **8** were made by reacting heterocyclic chlorides with amines (Scheme 1). Amino benztriazines **5** were made by exchange with the benztriazine thiol. With the more potent inhibitors described in this work, a 0.5:1 stoichiometry of inhibitor to enzyme (at elevated enzyme concentration) resulted in 50% inhibition of catalytic activity indicating indirectly the selectivity of the inhibitors for the active site.

Interaction with Asn131. Salicylamide **1a** has a $K_i = 0.05$ nM for SD. The R absolute configuration is necessary for potent inhibition and is identical to the configuration reported for the analogous amine portions of the commercial rice blast fungicide carpropamid (*30*). For the sake of comparison, Figure 2A includes salicylamide **1b** with a $K_i = 0.14$ nM. The additional fluorine of **1a** relative to **1b** increases potency approximately 3-fold. Salicylamide **1b** is, in turn, 5 times more potent than the quinazoline **2a** (Table 1), so minimal inhibitory potency is lost when going from the intramolecular hydrogen-bonded ring of a salicylamide to the heterocyclic ring of the quinazoline (see also ref *8*).

Quinazoline **2d** with the diphenylpropylamine substituent was 4.5 times more potent than the chiral bromo-α-methylbenzylamine substituent of **2a**. Hence, we chose to investigate both benzylamine and diphenylpropylamine substituents in the context of orienting a nitrile moiety to displace the crystallographic water molecule positioned between Try30 and Tyr50. It should be noted that SD inhibitors **1**−**7** have a well-positioned heteroatom to accept a hydrogen bond from the side-chain nitrogen of Asn131. Replacing the heteroatom with carbon decreases binding 80 times (compare **8d** with **5d**), highlighting the importance of this hydrogen bond to Asn131. The direct hydrogen bond between side chain amide nitrogen atom of Asn131 and the acceptor heteroatom would preclude trying to place substituents otherwise on the 3-position carbon of phthalazines **8** unless one believes the side chain of Asn131 could move substantially out of the way. Among numerous X-ray structures of SD in complex with different inhibitors, the side chain of Asn131 has remained relatively static (Z. Wawrzak, unpublished results). Furthermore, secondary hydrogen bonds from Ser129 and His133 with Asn131 would seem to anchor the position of the latter residue (Figure 2).

Table 1: Inhibition Constants of Amino Quinazolines **2**, Amino Quinolines **3** and **4**, Amino Benztriazines **5**, Amino Cinnolines **6** and **7** and Amino Phthalazines **8** for Scytalone Dehydratase

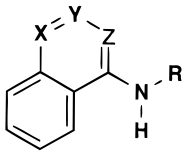

compd	X	Y	Z	R	K_i (nM)[a]
2a	N	CH	N	(*R*)-4-Br-α-Me-benzyl	0.68 ± 0.05
2d	N	CH	N	3,3-diphenylpropyl	0.15 ± 0.02
3d	N	CH	CH	3,3-diphenylpropyl	200 ± 40
4a	N	CH	C−CN	(*R*)-4-Br-α-Me-benzyl	0.25 ± 0.01
4d	N	CH	C−CN	3,3-diphenylpropyl	0.0066 ± 0.0009
5a	N	N	N	(*R*)-4-Br-α-Me-benzyl	1.2 ± 0.2
5d	N	N	N	3,3-diphenylpropyl	0.22 ± 0.02
6b	N	N	CH	4-Br-benzyl	2900 ± 170
6c	N	N	CH	4-Cl-benzyl	5500 ± 280
6d	N	N	CH	3,3-diphenylpropyl	140 ± 9
7a	N	N	C−CN	(*R*)-4-Br-α-Me-benzyl	0.35 ± 0.069
7b	N	N	C−CN	4-Br-benzyl	19 ± 2.0
7c	N	N	C−CN	4-Cl-benzyl	57 ± 4.6
7d	N	N	C−CN	3,3-diphenylpropyl	0.0077 ± 0.001
8b	CH	N	N	4-Br-benzyl	150 ± 5
8d	CH	N	N	3,3-diphenylpropyl	18.0 ± 1.2

[a] Values and standard errors.

Design of Inhibitors for Displacement of a Crystallographic Water Molecule. When there is an indirect, water-mediated hydrogen bond from an inhibitor to the protein, there is good reason to attempt to build into the space occupied by the water molecule. Computer models of SD complexed to **2a** (Figure 2B) and to **5a** (Figure 2C) were used as starting points for analysis and design. To determine the space around the bound inhibitor available for design, a Connolly solvent-accessible surface (Figure 4) was generated for the protein active site without the inhibitor **1a** and the two bound water molecules. Graphical analysis indicated that the space due to removal of the water molecule bound to tyrosines 30 and 50 could accommodate a small group. Our SD models suggested that the inhibitor's position labeled **X** in Figure 3 was the optimal place to project a small linear group such as a cyano group. This sp-hybridized group would project into the cavity formed by the bound water molecule providing favorable steric and polar properties. Cyanoquinoline **4a** was 2.5 times more potent as an SD inhibitor than the quinazoline analogue **2a**. More impressively, cyanoquinoline **4d** was over 20 times more potent than the analogous quinazoline **2d**. Thus, the nitrile functionality improved inhibitor binding despite the anticipated loss of the enthalpic contribution from the water molecule with the quinazoline 3-position nitrogen. The significance of this interaction was re-enforced by the performance of hydrogen-substituted quinoline **3d** which lost 30 000 times in binding potency relative to cyano-substituted **4d**. Our interpretation of the data is that the lone pair of electrons at the quinazoline 3-position is needed for the hydrogen-bonding network to

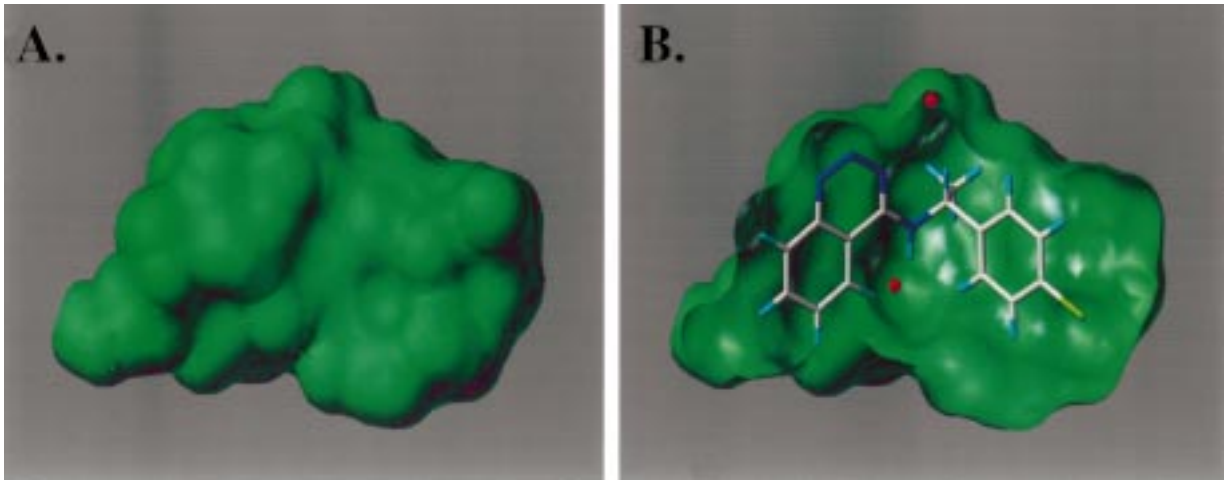

FIGURE 4: (A) Connolly surface of the SD-binding pocket generated from the crystal structure of the SD−1a complex. (B) The Connolly surface pealed partially back to expose the modeled benztriazine **5a** and the two associated water molecules (in red).

the water molecule. A carbon atom at the 3-position is disfavored when substituted with hydrogen because a hydrogen bond is lost, but it is favored when substituted with a nitrile due to the displacement of the water molecule.

This structure−activity correlation was also manifested in the series of benztriazine **5**, cinnoline **6** and cyanocinnoline **7** inhibitors. By replacing the 2-position carbon of quinazolines **2a** and **2d** with a nitrogen atom affording the corresponding benztriazines **5a** and **5d**, respectively, binding potency decreases only 1.5 times. We assume all the hydrogen-bonding interactions associated with the quinazoline would be maintained with the benztriazines. Cinnoline **6d** with a hydrogen atom displayed toward the bound water molecule is 600-fold less potent than **5d,** which has the available nitrogen lone pair of electrons, but when the nitrile is introduced as in **7d**, binding potency increases nearly 30-fold compared to **5d** and 18 000-fold compared to **6d**.

Placing a methyl group on benzylamine substituents increases inhibitory potency upward of 50 times (compare **7a** and **7b**). This is due in part to a favorable hydrophobic environment in the binding pocket for the methyl group and in part to the stabilization induced on the binding conformation of the benzyl substituent by favoring noneclipsing interactions in the nitrogen to phenyl bridge. Placing a methyl substituent analogously on 3,3-diphenylpropyl groups has been shown to diminish activity in the salicylamide analogue series. Extrapolating to the inhibitors described here, the negative effect of the methyl substituent is explained, retrospectively, by limited steric capacity as seen from the X-ray crystal structure of the SD−**7d** complex which we report in this work (vide infra). The bulkier diphenylpropyl group induces a realignment of some of the SD-binding pocket residues relative to the benzylamines, most notably manifested in Phe53. Other SD crystal structures have shown that, similar to this situation, some of the side-chain residues move due to the influence of different structural classes of SD inhibitors, but that the Cα trace of SD remains largely intact (Z. Wawrzak, unpublished results). The net result is that the diphenylpropyl substituent consistently confers greater binding potency than the bromo-phenethylamine substituent. Curiously, when there is a nitrogen atom displayed toward the binding pocket water molecule as in **2**, **5**, and **8**, the binding gain is relatively modest (4−5 times) compared to when there is a nitrile displacing the water molecule as in **4** and **7** (with a 35−45 times gain). We believe that the nitrile plays a role in predisposing the diphenylpropyl group toward its binding conformation by limiting some of the available degrees of rotational freedom in the relatively flexible bridge from the phenyl groups to the nitrogen atom.

*X-ray Crystallography of SD Complexed with **7d***. X-ray crystallographic data of the SD complex with **7d** has the nitrile occupying the position between Tyr30 and Tyr50 where the previous crystal structure (*6*) showed well-formed electron density which was appropriately assigned as a water molecule (Figure 5A). The high quality of the model is described by the statistics of Table 2. Resolution of 1.65 Å is a significant improvement over the 2.9 Å resolution of the original model, 1STD (*6*). The SD−**7d** crystals are in the *I*222 space group, the same as seen for three other SD−inhibitor complexes, and Ca^{2+} cations in this new structure have very similar interactions between trimers of SD in forming the crystal lattice as the others in this space group (Z. Wawrzak, T. Sandolova, J. Steffens, G. Basarab, T. Lundqvist, Y. Lindqvist, and D. Jordan, unpublished results). Electron density in the active site is excellent and definition of the inhibitor provided unequivocal assignment of its orientation. Key inhibitor−enzyme binding distances are shown in Figure 5B. The distances from the Tyr30 and Tyr50 side chain oxygen atoms to the inhibitor nitrile are 2.9 and 3.1 Å, respectively, giving credence to the notion that the nitrile π-electrons might pick up a weak interaction with the tyrosine hydroxyls (*16*). Neither of the tyrosines is well oriented geometrically to hydrogen bond to the sp-hybridized nitrile lone pair of electrons if one assumes that a 180° angle from the nitrile to the tyrosine hydroxyls would be ideal. No additional water molecules are seen within the region of the nitrile, and visual inspection of the region's Connolly surface (not shown) shows insufficient steric capacity to accommodate one. Given the high resolution of this structure, we can be quite confident that we succeeded in improving binding potency by displacement of the active-site water molecule.

As in the previous SD crystal structure (*6*), the water molecule associated with His85 and His110 remains well defined, 2.8 Å from the acyclic nitrogen atom of the inhibitor.

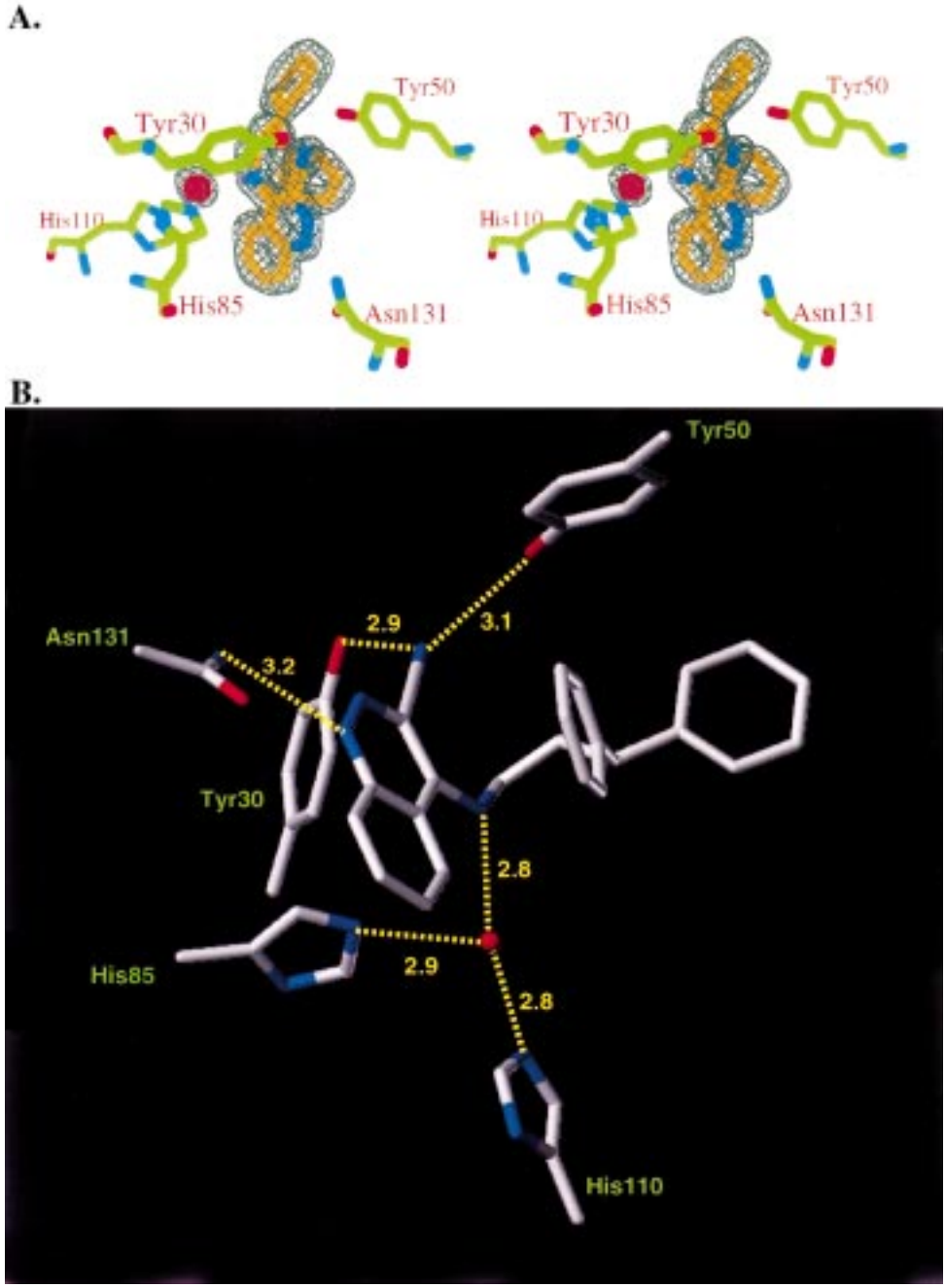

FIGURE 5: (A) Stereoview of the electron density map around inhibitor **7d** and the associated water molecule in the active site of scytalone dehydratase: $2|F_o| - |F_c|$. (B) Key contacts and distances (in angstroms) of **7d** with amino acid side chains of scytalone dehydratase.

A distance of 3.2 Å is seen between the Asn131 side-chain amide and the 1-position nitrogen atom of **7d**. The 1.65 Å resolution is insufficient to delineate between the 180° rotomers of the asparagine side chain amide, but the orientation shown in Figure 5B allows for donation of a hydrogen bond from the amide NH_2 to the inhibitor 1-position nitrogen atom.

CONCLUSIONS

The concept for design as outlined in Figure 3 was realized with the set of inhibitors described herein. Quinazolines such as **2a** and **2b** are quite potent inhibitors of SD. There is a water molecule within hydrogen-bonding distance to the 3-position nitrogen atom of quinazolines which we were able to displace by replacement of this nitrogen atom with a CN-substituted carbon atom. Inhibitor potency, resulting from this replacement, increases 2−20 times depending on the nature of the amine substituent. Similar results are seen when benztriazines **5a** and **5d** are modified to cyanocinnolines **7a** and **7d**. The high-resolution X-ray crystal structure of the SD−**7d** complex offers experimental verification of the water displacement. Molecules having a carbon atom at position 3 (Figure 3) that is substituted with a hydrogen atom were markedly less potent (by factors of 100−18000) inhibitors of SD. The poorer binding affinity of these hydrogen-substituted inhibitors is attributed to the hydrogen atom being too small to displace the water molecule being held by Tyr30 and Tyr50 and to an unfavorable interaction between the hydrogen atom and the same water molecule that remains in place.

Table 2: Statistics for Data Collection and Refinement of SD in Complex with **7d**[a]

parameter	values	parameter	values
(A) internal merging and scaling		(B) refinement	
resolution (Å)	20.40−1.65	resolution (Å)	8.0−1.65
space group	*I*222	reflections [$F_o > 2\sigma(F_o)$]	65 428
cell dimensions (Å)	80.23, 90.26, 162.14	*R*-factor (%)	19.4
	$\alpha = \beta = \gamma = 90°$	*R*-free (%)	23.0
V_M [Å^3/(Da)]	2.52		
water content (%)	51.2		
		(C) geometry and deviations	
no. of reflections	512 109	no. of protein atoms	4104
no. of unique reflections	66 465	no. of water molecules	411
R-merge	0.058	mean *B* (Å^2)	18.1
completeness (overall) (%)	93.7	rmsd bond distances	0.009
completeness (last shell) (%)	86.4.	rmsd bond angles	1.415
$I/\sigma(I)$	29.2	rmsd torsion angles	24.50
		rmsd impropers	1.269

[a] *R*-merge $= \sum_{hkl}\sum_i(I_i - \langle I\rangle)/\sum_{hkl}\sum_i(\langle I\rangle)$, where I_i is the scaled intensity to the ith observation, $\langle I\rangle$ is the mean intensity of this reflection.

The increases in inhibitory potency mediated by introduction of the CN moiety into this class of chemistry can be ascribed to contributions from at least three factors: the entropy gain by the release of water to bulk solvent, the entropy gain due to the ortho-CN limiting conformational mobility of the amine substituent, and the augmentation of the enthalpic binding between the inhibitor and protein. There is a challenge associated with generating a scaffold that allows for building into water-occupied regions of proteins to gain the benefits of water displacement. There is also a challenge associated with finding the correct functionality that can favorably interact with the residues otherwise associated with the water molecule.

Recently, there was a report in which a heterocyclic NH was changed to COH in an attempt to displace a crystallographic water molecule seen in the crystal structure of hyperzine A bound to *Torpedo* eel acetylcholinesterase (*9*). The net replacement of H with OH did not suffice to displace the water molecule as determined by binding studies presumably because the OH substituent was insufficiently large to extend into the pocket occupied by the water molecule. This is analogous to replacing the nitrogen lone pair of quinazolines such as **2d** with the hydrogen atom of quinolines such as **3d** which decreased binding potency toward SD. What we have shown to be required is a larger substituent such as CN which extends further into the space occupied by the vacated water molecule. In our case, the cinnoline and quinoline scaffolds proved to be quite valuable relative to salicylamide **1a** in achieving our objective of correctly displaying the CN functionality for water displacement.

ACKNOWLEDGMENT

We thank Rand Schwartz, Steve Hansen, Troy Gehret, and Matthew Scheideman for excellent technical assistance. Frank Hollinger (Wyeth-Ayerst Research) is gratefully acknowledged for reading of this manuscript.

REFERENCES

1. Babine, R. E., and Bender, S. L. (1997) *Chem. Rev. 97*, 1359−1472.
2. Marrone, T. J., Briggs, J. M., and McCammon, J. (1997) A. *Annu. Rev. Pharmacol. Toxicol. 37*, 71−90.
3. Bell, A. A., and Wheeler, M. H. (1986) *Annu. Rev. Phytopathol. 24*, 411−415.
4. Chumley, F. G., and Valent, B. (1990) *Mol. Plant-Microbe Interact. 3*, 135−143.
5. Howard, R. J., and Ferrari, M. A. (1989) *Exp. Mycol. 13*, 403−418.
6. Lundqvist, T., Rice, J., Hodge, C. N., Basarab, G. S., Pierce, J., and Lindqvist, Y. (1994) *Structure (London) 2*, 937−944.
7. Zheng, Y.-J, and Bruice, T. C. (1998) *Proc. Natl. Acad. Sci. U.S.A. 95*, 4158−4163.
8. Hodge, C. N., and Pierce, J. (1993) *Bioorg. Med. Chem. Lett. 3*, 1605−1608.
9. Campiani, G., Kozikowski, A. P., Wang, W., Ming, L., Nacci, V., Saxena, A., and Doctor, B. P. (1998) *Biorg. Med. Chem. Lett. 8*, 1413−1418.
10. Lam, P. Y. S., Ru, Y., Jadhav, P. K., Aldrich, P. E., DeLucca, G. V., Eyermann, C. J., Chang, C.-H., Emmett, G., Holler, E. R., Daneker, W. F., Li, L., Confalone, P. N., McHugh, R. J., Han, Q., Li, R., Markwalder, J. A., Seitz, S. P., Sharpe, T. R., Bacheler, L. T., Rayner, M. M., Klabe, R. M., Shum, L., Windslow, D. L., Kornhauser, D. M., Kackson, D. A., Erickson-Viitanen, S., and Hodge, C. N. (1996) *J. Med. Chem. 39*, 3514−3525.
11. Vara, Prasad, J. V. N., Lunney, E. A., Ferguson, D., Tummino, P. J., Rubin, J. R., Reyner, E. L., Stewart, B. H., Guttendorf, R. J., Domagala, J. M., Suvorov, L. I., Gulnik, S. V., Topol, I. A., Bhat, T. N., and Erickson, J. W. (1995) *J. Am. Chem. Soc. 117*, 11070−11074.
12. Romines, K. R., Watenpaugh, K. D., Howe, W. J., Tomich, P. K., Lovasz, K. D., Morris, J. K., Janakiraman, M. N., Lynn, J. C., Horng, M.-M., Chong, K.-T, Hinshaw, R. R., and Dolak, L. A. (1995) *J. Med. Chem. 38*, 4463−4473.
13. Bryan, W. P. (1994) *Science 266*, 1726.
14. Dunitz, J. D. (1994) *Science 264*, 670.
15. Krantz, A. (1992) *Bioorg. Med. Chem. Lett. 2*, 1327−1334.
16. Nishio, M., Umezawa, Y., Hirota, M., and Takeuchi, Y. (1995) *Tetrahedron 31*, 8665−8701.
17. Lundqivst, T., Weber, P. C., Hodge, C. N., Braswell, E. H., Rice, J., and Pierce, J. (1993) *J. Mol. Biol. 232*, 999−1002.
18. Thompson, J. E., Basarab, G. S., Pierce, J., Hodge, C. N., and Jordan, D. B. (1998) *Anal. Biochem. 256*, 1−6.
19. Chen, J. M., Sheldon, A., and Pincus, M. R. (1995) *J. Biomol. Struct. Dyn. 12*, 1129−1159.
20. Abbott, P. J., Acheson, R. M., Kornilov, M. Y., and Stubbs, J. K. (1975) *J. Chem. Soc., Perkin Trans. 1 22*, 2322−2326.
21. Eggert, K., Heber, D., and Ravens, U. (1990) *Arch. Pharm. 323*, 611−618.
22. Stevens, H. N. E., and Stevens, M. F. G. (1970) *J. Chem. Soc. C 6*, 765−771.
23. Turck, A., Ple, N., Tallon, V., and Queguiner, G. (1995) *Tetrahedron 51*, 13045−13060.
24. Ames, D. E., and Bull, D. (1981) *Tetrahedron 37*, 2489−2491.
25. Segel, I. H. (1975) *Enzyme Kinetics*, John Wiley & Sons, New York.

26. Navaza, J. (1994) *Acta Crystallogr., Sect. A 50*, 157−163.
27. Brünger, A. T., Kuriyan, J., and Karplus, M. (1987) *Science 235*, 458−460.
28. Brünger, A. T., Krukowski, J., and Erickson, J. (1990) *Acta Crystallogr., Sect. A 46*, 585−593.
29. Brünger, A. T. (1992) *Nature 355*, 472−475.
30. Kurahashi, Y., Sakawa, S., Kinbara, T., Tanaka, K., and Kagabu, S. (1997) *J. Pestic. Sci. 22*, 108−112.

BI981848R